PAPER • OPEN ACCESS

Simulations of ICRF heating of fusion oriented plasmas in plane-stratified and full toroidal geometry

To cite this article: M. Brambilla and R. Bilato 2021 *Nucl. Fusion* **61** 076016

OPEN ACCESS
IOP Publishing | International Atomic Energy Agency Nuclear Fusion
Nucl. Fusion **61** (2021) 076016 (11pp) https://doi.org/10.1088/1741-4326/ac0128

Simulations of ICRF heating of fusion oriented plasmas in plane-stratified and full toroidal geometry

M. Brambilla* **and R. Bilato**

Max Planck Institute for Plasma Physics, Boltzmannstr. 2, 85748 Garching, Germany

E-mail: Marco.Brambilla@ipp.mpg.de

Received 19 February 2021, revised 5 May 2021
Accepted for publication 13 May 2021
Published 17 June 2021

Abstract

We compare results from the fully toroidal TORIC–SSFPQL package (Brambilla and Bilato 2006 *Nucl. Fusion* **46** s387) and from the plane-stratified geometry solver FELICE (Brambilla 1989 *Plasma Phys. Control. Fusion* **31** 723) to illustrate the advantages and the limitations of the two approaches for the simulations of Ion Cyclotron Radio Frequency heating of tokamak plasmas. We point out that some of the predictions of the plane-stratified models do not straightforwardly apply to the true toroidal configuration. This is the case, in particular, for the excitation of guided modes between the plasma surface and the vessel.

Keywords: tokamak, radio-frequency heating, ICRF, full wave, slab, toroidal

(Some figures may appear in colour only in the online journal)

1. Introduction

A considerable number of codes are by now available for the numerical simulation of radio frequency (RF) heating of tokamak plasmas in the ion cyclotron (IC) range of frequencies, important both for the understanding of present day experiments, and for the planning of the auxiliary heating system in ITER and DEMO. In addition, several codes have been developed for the investigation of the interactions of the RF waves with the plasma in the scrape-off layer (SOL) and with metallic obstacles (Faraday screen, antenna, vessel). Our considerations will concern mainly 'global' codes aiming at predicting the interactions with the plasma core: power deposition profiles, heating rates, distribution functions of the heated species, etc; because of their importance for the success of RF auxiliary heating, however, a few comments will be devoted also to the other group of codes. Global codes can be neatly divided into two categories, namely very fast codes which achieve their performances by assuming that only the 'horizontal' variations of the plasma parameters (density, temperature, magnetic field intensity) along the equatorial plane are of importance, and much slower codes taking into account toroidicity in full. For simplicity, we will refer somewhat loosely to the former as slab geometry codes, and to the latter as toroidal codes. From the literature, one gets the impression that it is not always clear what each kind of code can do, and what their limitations are. We think it therefore appropriate to offer a few comments on the situation. It is not possible for this limited purpose to discuss all the work which has been done in this field, and we will limit our considerations to a few but significant examples.

Among the available toroidal codes, at least three, namely AORSA [1–3], EVE [4, 5], and TORIC [6, 7], solve the wave equations in full toroidal geometry using models which cover most of the physics involved:

- In these codes, the dielectric response is evaluated for a hot plasma, so that they describe IC absorption at the fundamental and its first harmonic, absorption by electrons including electron landau damping (ELD), transit time damping (TTMP) and the mixed term [8], as well as mode conversion (MC) to ion Bernstein waves (IBW) or to the IC wave (ICW) (cf section 2).

* Author to whom any correspondence should be addressed.

- Two of these codes, namely AORSA and TORIC actually solve wave equations valid to all order in the ratio of the thermal ion Larmor radius to the local wavelength, although not in the integro-differential form which follows from the integration of the linearized Vlasov equation [9, 10]. For this purpose AORSA [1] represents the fields of each independent toroidal Fourier component as a two dimensional superposition of plane waves, assuming that each partial wave locally satisfies the uniform hot plasma dispersion relation corresponding to its wavevector, with correction of first-order for the non-uniformity of the toroidal configuration. TORIC represents the fields as a Fourier superposition of toroidal and poloidal modes, writing the wave equations in the plasma in the partial differential form which is obtained from Vlasov equation expanding to second order in the Larmor radius [11–13], but the coefficients of the wave equations are corrected for large Larmor radius effects whenever required to evaluate ELD of IBWs excited by mode conversion, damping of the fast wave (FW) at IC harmonics higher than the first, and the contributions to the plasma response of thermonuclear alpha particles in slowing-down [14–16]. In this context it is worth mentioning that although large Larmor radius effects require the evaluation of a large number of modified Bessel functions, the algorithms available for this purpose are so efficient that this takes a negligible fraction of the execution time.
- These codes are coupled to a solver of the bounce-averaged quasilinear (QL) kinetic equation (valid when for most ions it is possible to neglect the radial excursions of their orbits): AORSA with CQL3D [3], EVE with AQL [5], and TORIC with SSFPQL [17]; TORIC has also been coupled to a reduced version of CQL3D [18].
- AORSA [2, 3] and TORIC [19–21] evaluate the coefficients of the wave equations taking into account the deviations of the ion distribution functions from local thermal equilibrium, as calculated by the kinetic solver in a self-consistent way (cf section 4).
- The TORIC–SSFPQL package includes the code SINBAD [22]; this makes it possible to describe the synergy between ICRF heating with neutral beam injection (NBI) [21].

Solvers of the wave equations in plane-stratified geometry [13, 23–25] execute orders of magnitude faster than toroidal ones, and allow for a more detailed modeling of the SOL and the antenna. They are therefore useful, in the first place, for the evaluation of the performance of IC antennas, and as tools in the investigation of the interactions between RF fields and the SOL and with the metallic vessel. A version of the slab finite element solver FELICE [13] is used in the antenna code TOPICA [26, 27], but FELICE itself has only a rather simple antenna model, which differs from that of TORIC only because FELICE takes into account the presence of the radial conductors from feeders and shorts to the active straps parallel to the plasma surface. Actually, as elements of an antenna code, solvers simpler than FELICE can be even more appropriate: by taking into account only the FW, and by imposing outward radiation conditions at some surface closer to the antenna than any singular surface (IC or ion-ion resonances) in the plasma, slab geometry codes can be made less prone to predict the excitation of spurious cavity modes, which falsify the estimates of the antenna load and of the amplitude of the fields in the near field region. An excellent example of this approach is the ANTITER code [23].

Slab solvers can be useful also for a first orientation when interpreting or planning ICRF heating experiments; their value for this purpose, however, is somewhat limited by the fact that so far no significant effort has been made to prove that their predictions do not differ much from those of fully toroidal codes. On the contrary, in the presentation of some of these codes the possibility of simulations in toroidal geometry is not even mentioned. It is important, however, to be aware of several reasons to regard some of the results obtained from slab geometry codes as only qualitative.

- In plane-stratified geometry waves reflected from the plasma surface, or internally, e.g. at ion-ion cutoffs, are fully coherent with the incident wave launched by the antenna. This tends to overestimate the importance of weakly damped eigenmodes both in the vacuum region around the plasma, and inside the plasma itself. In scenarios with low 'absorption per transit' strong excitation of such modes can make the slab geometry solution almost meaningless. In toroidal geometry the different topology, the curvature of magnetic surfaces, and the poloidal inhomogeneity of the confining magnetic field drastically reduce the quality factor of any residual cavity mode.
- An other example of toroidal effect which is lost in slab simulations is 'focussing' of the launched waves by the convexity of the magnetic surfaces. This effect becomes important in large plasmas with more or less total absorption in a single transit.
- It is impossible to map unambiguously the power deposition profiles obtained by integrating the wave equations in a plane-stratified plasma model onto the magnetic surfaces of the real tokamak configuration, despite a few attempts in the past [28, 29]. Slab geometry codes, therefore, cannot make available to the solver of the QL kinetic equation the minimal information required, namely the power absorbed per ion on each magnetic surface, in order to allow a truly self-consistent evaluation of the deviations of the ion distribution functions from Maxwellian due to IC heating, and of the influence of these deviations on wave absorption.
- When coupled to a solver of the Fokker–Plank (FP) QL kinetic equations, slab geometry codes can maintain their speed of execution only if the FP equation is also made one-dimensional (1D) by integrating over the perpendicular degrees of freedom, as pioneered by Stix [8]. The comparison of the results obtained with a solver of the reduced 1D FP equation, and those from a full velocity-space solver or from experimental measurements easily shows, however, that the 1D kinetic equation gives good

results only at very low RF power density, and in very collisional plasmas, for example in the Princeton large torus [30]. At higher power, and/or for less collisional plasmas, the anisotropy of the suprathermal populations produced by ICRF heating is such a dominant feature that it cannot be just integrated over.

In the following sections we illustrate these considerations with a few examples. In the next section we compare a series of simulations performed with TORIC–SSFPQL with the same simulations performed with the slab geometry solver FELICE. Section 3 is devoted to a somewhat more detailed discussion of the role of surface, waveguide, and cavity modes in slab and toroidal geometry. In section 4 the SSFPQL kinetic solver is used to show the importance of iterating this code with the solver of the wave equations taking into account the anisotropy of the QL distribution functions to achieve a self-consistent picture of ICRF heating of tokamak plasmas.

Before turning to the examples, it is fair to say a few words also on a technical limitation of toroidal solvers, and on the specialized codes which are used to overcome this limitation in view of improving our understanding of the interactions of RF waves in the IC range of frequency with the SOL and the antenna. In the conclusions we will also mention a few unsolved problems concerning the physics of RF heating which still limit the predictive value of toroidal codes, and which deserve, in our opinion, more attention than is currently devoted to their solution.

In the first place, we may note that there is no obstacle to take into account a realistic SOL in slab codes: both FELICE and ANTITER (and other codes as well) have this facility, and the latter code has been used for interesting investigations of parasitic losses in this region, in particular at the transit through the lower hybrid (LH) resonance [31]. Also TORIC can optionally take into account an SOL plasma outside the last closed surface; but in toroidal geometry the flexibility of SOL modelling is limited by the increasingly high demands on the discretization mesh to maintain sufficient accuracy as the density and temperature decrease to very low values.

This is one of the reason why the antenna model is almost inevitably more idealized in toroidal than in slab codes. But there is an even simpler practical reason. Exploiting axisymmetry, the normal procedure to perform a complete simulation is to begin by solving separately the wave equations for N toroidal Fourier modes: this step requires information only on the poloidal distribution of the currents in the antenna, and can be easily parallelized. Then one superposes the results taking into account the geometry of the antenna in the toroidal direction. This implies, however, that the dependence on the toroidal and poloidal angle of the distribution of the antenna currents must be 'factorized', say $J(\vartheta, \varphi) = G(\varphi)H(\vartheta)$ (all straps identical and in the same magnetic surface, the excitations differing only in the phase configuration of the straps). It is fortunate that the sensitivity of the results important for auxiliary heating and current drive (power repartition among species, power deposition profiles) to the details of the current distribution in the poloidal direction is weak enough to justify this approach; but a detailed study of the SOL and antenna regions is excluded.

Investigations of RF interactions with the wall and metallic obstacles require a different approach also because they must account for details (localized Faraday screen, image currents in septa and lateral protections of the antenna, etc) which break axisymmetry. This makes it necessary to discretize the wave equations in all three dimensions, abandoning the convenient Fourier decomposition in the ignorable coordinates used in global solvers. In turn, however, this restricts the plasma model to the strictly cold limit, and wave absorption to collisional damping.

A way to overcome this limitation is to use the surface impedance matrix (SIM) of the core plasma, as suggested by Shiraiwa *et al* [32] to connect the solution in hot core region, obtained with TORIC, to the solution in the SOL, where the wave equations can be solved on a three-dimensional mesh. The introduction of the SIM is natural in plane stratified geometry, and is the technique used in FELICE to connect the numerical solution in the plasma to the solution in vacuum, which is obtained analytically [33, 34]. In toroidal geometry, however, it is an extremely computationally demanding approach: if a converged simulation of the core region requires N toroidal Fourier modes and for each of them M poloidal Fourier modes, the SIM is a symmetric complex matrix of $2 \times N \times M$ rows and columns; the number of independent runs of TORIC required to evaluate all its elements is simply prohibitive (Shiraiwa *et al* have evaluated the SIM for a single representative toroidal mode, which is already a feat). An additional problem is the already mentioned relative insensitivity of the core solution to the details of the poloidal current distribution, and the very different launching efficiency of a driving electric field oriented toroidally or poloidally: evaluating and using the SIM to solve the concrete global problem is likely to be a very 'stiff' task, greatly amplifying the unavoidable numerical errors of the individual runs of TORIC.

For this reasons, investigations of the SOL and antenna region, in particular to obtain detailed information of the fields in the antenna region, which can be responsible for sputtering and impurity generation, are currently made with specialized codes of a different type, which discretize the cold plasma wave equations only in an appropriate rectangular region representing the layer between the wall and the surface of the hot plasma. These codes are outside the scope of the present note, but one consideration might be added. The boundary conditions imposed at the far end of the integration domain are necessarily of the 'outward radiation' (OR) type (no power coming toward this surface from the core plasma). This is the case, for example, in the case of RAPLICASOL [35], based on the commercial software COMSOL [36]. This condition is equivalent to the OR condition which can be imposed in FELICE at some distance from the plasma edge, before any singular layer (cutoffs, wave or IC resonances) in the plasma. The Fourier spectra of the fields predicted both by FELICE when integrating over the full plasma cross-section, and by TORIC, however, are often quite different, as will be shown in section 4. As a consequence, there is no simple way of using

the output of one of these codes as input for a global toroidal solver, in order to produce simultaneously realistic simulations of the SOL and the antenna on the one hand, and of the core plasma on the other hand: this would require the knowledge of the SIM, as attempted by Shiraiwa *et al*. This is probably not a serious drawback; the question remains open, however, how much the different fields expected when power reflected back from singularities in the core plasma is taken into account do influence the fields near the antenna, whose knowledge is the goal of the simulations with COMSOL.

2. Solving the wave equations in plane-stratified and toroidal geometry

To compare TORIC and FELICE we have chosen a typical minority scenario (hydrogen minority in deuterium) in a medium size tokamak (major and minor radius $R = 1.65$ m and $a = 0.48$ m, values on axis $B_0 = 2.5$ T, $n_e = 6 \times 10^{19}$ m^{-3}, $T_e = T_i = 4.2$ keV; the applied frequency has been assumed to be 35 MHz, putting the IC resonances about 10 cm to the low field side of the magnetic axis), and we have varied the minority concentration between zero and 25%, thereby covering both the minority and the mode conversion regimes (in this case the transition occurs roughly at $n_H/n_e \simeq 0.10$). Since for the reasons which will be clear below we do not regard it meaningful to couple the 1D code FELICE to a QL kinetic solver, in this section we have limited ourselves to the case of Maxwellian distribution functions also in the runs of TORIC.

In a device of this size the typical toroidal power spectrum of a two-strap antenna excited in the antisymmetric configuration extends roughly to $-35 \lesssim n_\varphi \lesssim +35$, and a well-converged run of TORIC requires 31 poloidal modes, $-15 \leqslant m_\vartheta \leqslant +15$ for each toroidal mode; the runs of FELICE have been made with the same number of Fourier components. It might be of some interest that on a laptop for these simulations each run of FELICE executes in about 10s, while the same run of TORIC lasts somewhat less than half an hour; the CPU time of TORIC, however, is drastically reduced on a mainframe thanks to the parallelization in the toroidal mode numbers.

Figures 1 and 2 show the global power repartition predicted by the two codes as a function of the minority concentration. The most conspicuous difference is the m uch larger electron absorption predicted by FELICE, at the expense of ion heating. Since in the case of a Maxwellian plasma the two codes solve exactly the same wave equations, the reason is to be found in the different geometry. Discretizing the poloidal wavenumber in FELICE in the same way as in TORIC means that in the former code the plasma cross-section is implicitly assumed to be rectangular, instead of roughly elliptical, as it really is. As a consequence, in FELICE the FW appears to traverse a much larger plasma volume than in TORIC before reaching the IC resonances, in which it is exposed only to damping by the electrons.

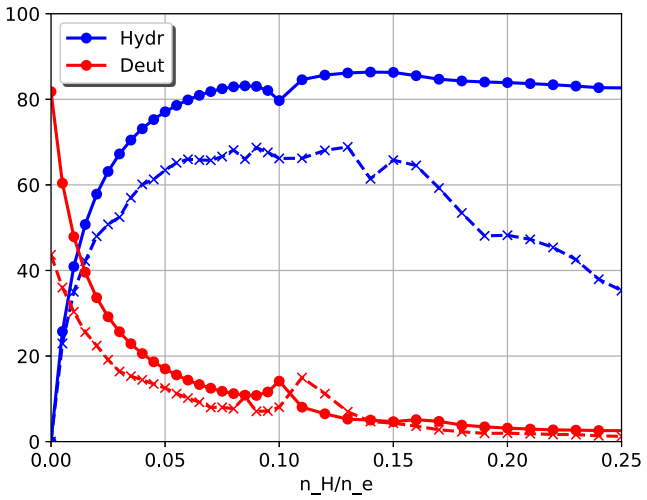

Figure 1. Fraction of power absorbed by the ions versus hydrogen concentration. Dashed lines with crosses: FELICE code; full lines with dots TORIC.

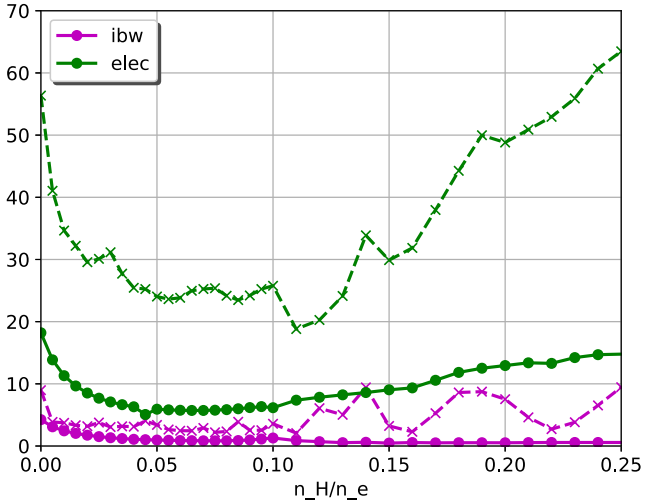

Figure 2. Fraction of power absorbed by electrons, including the power mode converted to IBW versus hydrogen concentration. Dashed lines with crosses: FELICE code; full lines with dots TORIC.

FELICE also predicts an appreciably higher efficiency of mode conversion to IBWs, particularly in the mode conversion regime in which, according to TORIC, the mode converted power decreases below 1% as the optical thickness of the evanescence layer associated with the ion–ion cutoff increases, and screening of E_+ by minority ions begins to play an increasing role. In toroidal geometry mode conversion to IBWs can occur only in a relatively narrow layer around the equatorial plane; above and below mode conversion is instead to the ICW [37, 38], a form of the shear wave close to the transition to a parallel propagating whistler. This kind of mode conversion requires a gradient of the static magnetic field intensity along magnetic field lines, and, therefore, is not possible in plane stratified geometry. Thus FELICE predicts a uniform excitation of IBW across the whole height of the plasma. In the mode conversion regime, moreover, absorption

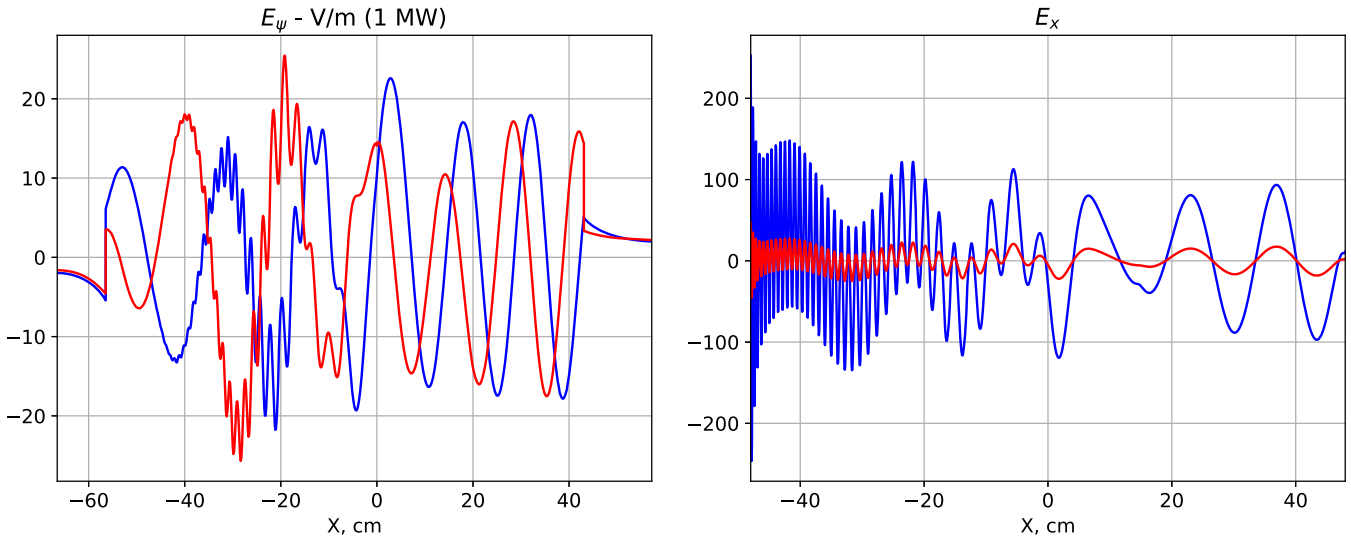

Figure 3. Radial component of the RF electric field along the equatorial plane, $n_\varphi = 12$, $n_H/n_e = 0.03$. Left: E_ψ (TORIC); right: E_x (FELICE).

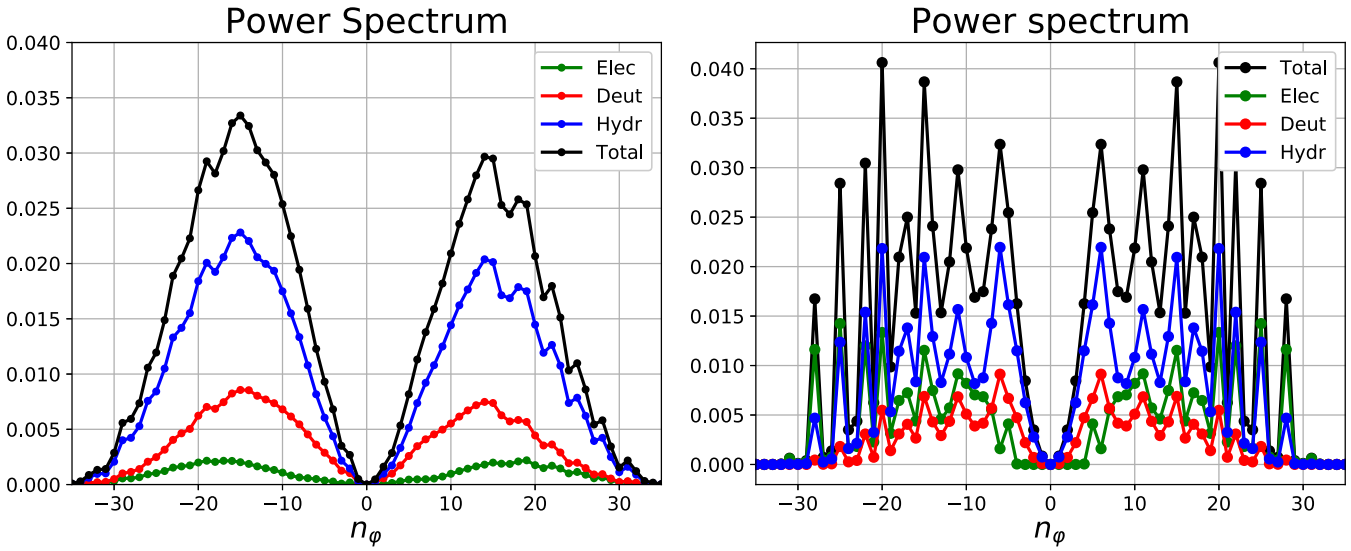

Figure 4. Toroidal power spectrum (normalized to unit), $n_H/n_e = 0.03$. Left TORIC; right: FELICE.

per transit is appreciably weaker than in the minority regime: as a consequence, in FELICE multi-transit partly compensates for the increased opacity of the evanescence layer and the increased $|E_+|^2$ screening, maintaining a higher level of mode conversion efficiency, with oscillations depending on whether a maximum or a node of the FW field amplitude occurs at the mode conversion layer. In toroidal geometry the coherence between incoming and reflected wave required for this effect is largely lost. Once the IBW is excited, moreover, its propagation is very different in the two geometries: in reality and in TORIC, but not in FELICE, this short wavelength mode is subject to strong refraction, which tends to rapidly increase the local value of $k_\parallel$, and thus to accelerate the onset of electron Landau damping [37]. This is illustrated in figure 3 for the toroidal mode $n_\varphi = 12$, $n_H/n_e = 0.03$ (for this particular case the two codes agree in predicting a mode conversion efficiency of somewhat less than 5% in power): according to TORIC the IBW is fully absorbed well before reaching the inner plasma edge, while according to FELICE it has a much larger amplitude, and propagates essentially undamped in the whole high-field half of the plasma.

The tendency of plane-stratified geometry to overestimate the effects of coherent interference between incoming and reflected waves is clearly illustrated in figure 4. One of its consequences is that the toroidal power spectrum predicted by FELICE is much more irregular and spiky than the spectrum predicted by TORIC. The spikes correspond to weakly damped internal eigenmodes between the outer plasma boundary and the ion–ion cutoff (not to be confused with the surface eigenmodes discussed in the next section); they are more marked in the domain of larger toroidal wavenumbers, for which IC absorption is somewhat weaker and (in FELICE but not in TORIC) electron damping dominates. Internal eigenmodes of

this kind are present also in the TORIC solution, but with a substantially lower quality factor.

3. Surface, waveguide, and cavity modes between plasma and vessel

Particularly annoying for slab solvers are modes guided between the plasma surface and the metallic vessel, that form a virtual plane waveguide infinite in both the toroidal and poloidal direction. Spurious excitation of these modes can negatively affect the estimate of the antenna load, and of the intensity of the near RF fields. In the limit in which the vessel is very far from the plasma edge these modes are surface modes guided by the plasma surface; Tierens and Colas [39] have pointed out that the dispersion relation of these modes is

$$\det\left(\underline{\underline{Z}}_p - \underline{\underline{M}}\right) = 0 \tag{1}$$

where

$$\underline{\underline{M}} = \frac{1}{n_x}\begin{pmatrix}(1-n_y^2) & -n_y n_z \\ -n_y n_z & (1-n_z^2)\end{pmatrix} \quad \begin{matrix} n_x^2 = 1-(n_y^2+n_z^2) \\ \vec{n} = (\omega/c)\vec{k}\end{matrix} \tag{2}$$

is the vacuum impedance matrix ($n_x \to \pm i(-n_x^2)^{1/2}$ for partial waves evanescent in vacuum, depending on the direction of evanescence), and $\underline{\underline{Z}}_p$ is the surface impedance matrix of the plasma, evaluated by FELICE (for the definitions of these matrices cf [34]). In reality, the vessel is always at a distance from the plasma much shorter than one vacuum wavelength, and its presence cannot be ignored; the spurious modes are therefore waveguide modes. To take this into account it is sufficient to replace the vacuum impedance matrix with the impedance matrix of a metallic wall as seen from the plasma surface

$$\underline{\underline{Z}}_w = i \tan k_x d\, \underline{\underline{M}}, \tag{3}$$

where d is the distance between the plasma surface and the wall. In contrast to surface modes, waveguide modes can have also $n_x^2 > 0$. In the limit $\underline{\underline{Z}}_p \to 0$ they become the TE eigenmodes of an infinite plane metallic guide, which transport power to infinity in the direction defined by the wavenumbers n_y and n_z; the plasma side of this guide, however, is leaky, so that this power finally enters the plasma.

Since even in slab solvers n_y and n_z are discretized to simulate the double periodicity of the torus ((in FELICE $k_y = m_\vartheta/b$ and $k_z = n_\varphi/(R+a)$, with a and R the minor and major radius, and b/a the elongation of the plasma surface), the probability of a couple (n_y, n_z) exactly coinciding with those of a waveguide eigenmode is practically zero. Some of the partial waves with (n_y, n_z) close to those of such an eigenmode, however, are 'resonantly' driven to a large amplitude, and their presence manifests itself in the large spikes visible in the power spectra predicted by FELICE and similar slab solvers. This is illustrated in figure 5, left. In this case the run of FELICE used an ITER high performance scenario [40] with $n_e(0) = 1.2 10^{20}$ m^{-3}, $T_e(0) = T_i(0) = 9.9$ keV, 46% deuterium, 50% tritium, 2% helium3; the frequency was assumed 53 MHz, with the four straps excited in the $(0, \pi, 0, \pi)$ configuration. Outward radiation conditions (ORCs) were imposed 30 cm inside the plasma.

A peculiar feature of this figure is the absence of spikes in the immediate vicinity of $n_z = 0$ (this is true independent of the phase configuration of the straps). Thus there is an important difference between an infinite guide with two metallic walls and the virtual guide of the simulated tokamak, in which one metallic wall is replaced by the plasma surface. In the former the poloidal and toroidal directions would be completely equivalent; in the second, by contrast, only modes with $0.6 \lesssim \mathrm{mod}\, n_z \lesssim 1.2$ are excited, and for each n_z the poloidal number with largest amplitude is the one which corresponds to the smaller value of n_x^2. Eigenmodes propagating in the toroidal direction are completely suppressed. This is confirmed by running FELICE for the same scenario, but with only the partial wave $n_y = 0$: (figure 5, right): the spectrum obtained is perfectly smooth.

Of course, the real configuration is finite both in the poloidal and the toroidal directions; hence in the tokamak neither surface nor waveguide modes are possible, but only cavity modes. These modes are much more constrained than waveguide modes; in addition, the cavity between plasma and vessel in a torus has an unusual topology, and, because of the poloidal inhomogeneity of the equilibrium, the boundary conditions on the plasma side are much more complicated than in slab geometry. Except in scenarios with very weak absorption (e.g. current drive experiments with absorption only by electrons), therefore, the quality factor of the eigenmodes of this cavity is likely to be rather poor. Hence one can anticipate that the occurrence of a strongly driven resonance between one of these eigenmodes and a Fourier component of the fields excited by the IC antenna is very unlikely. This is consistently confirmed by simulations in toroidal geometry: in the solutions obtained from TORIC the fields in vacuum are practically never much larger than in the plasma.

Exploiting the characteristics of guided modes mentioned above, we have implemented in FELICE a heuristic method to recognize spurious eigenmodes and subtract their contribution from the launched spectrum and from the antenna load. In the case of the ITER scenario considered here, this reduces the load from 0.745 to 0.546 Ω per strap; and the toroidal power spectrum 'filtered' for spurious surface guided mode (figure 6 left) is indeed very similar to the one of figure 5, right, and also to the spectrum obtained from TORIC (figure 6, right; note, however, that the spectrum of FELICE is obtained imposing ORCs 30 cm inside the plasma, while the solution of TORIC is always global; for the reasons explained in the previous section, it is impossible to make FELICE agree with TORIC while integrating over the entire plasma). In principle, one could subtract the contribution of spurious guided modes also from the power deposition profiles from FELICE; this, however, is very cumbersome, and hardly worthwhile, in view of the heuristic nature of the approach, and the availability of simulations in toroidal geometry.

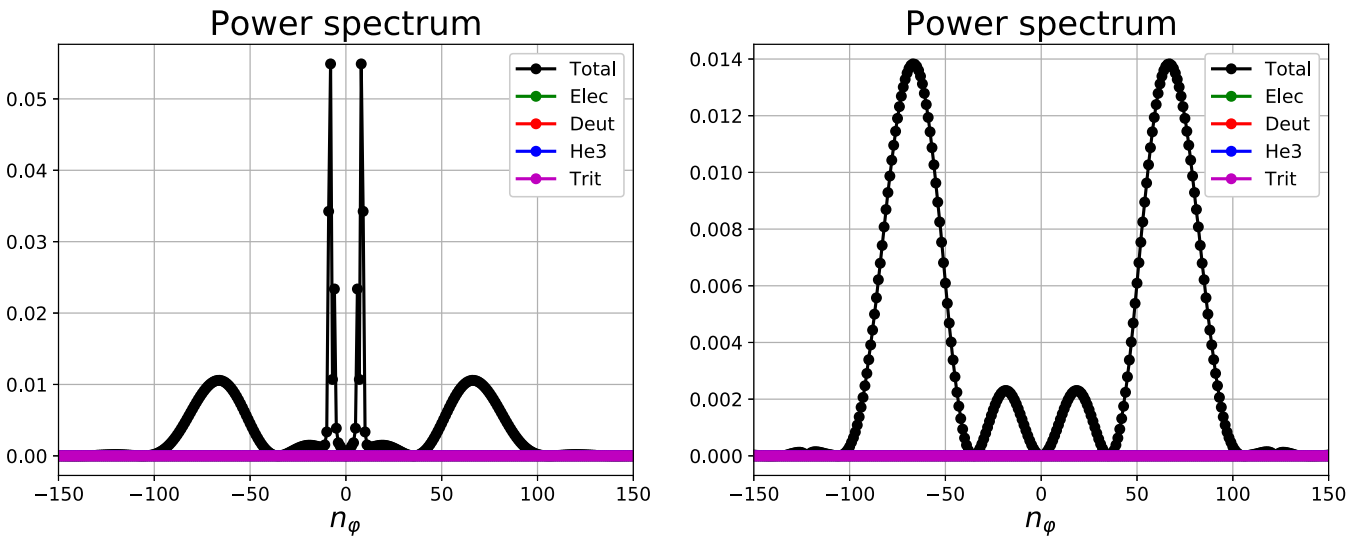

Figure 5. Toroidal power spectrum predicted by FELICE for the ITER antenna in the $(0, \pi, 0, \pi)$ configuration. Left: poloidal modes in the range $-2.87 \leqslant n_y \leqslant +2.87$ $(-15 \leqslant m_\vartheta \leqslant +15)$. Right: only $n_y = 0$.

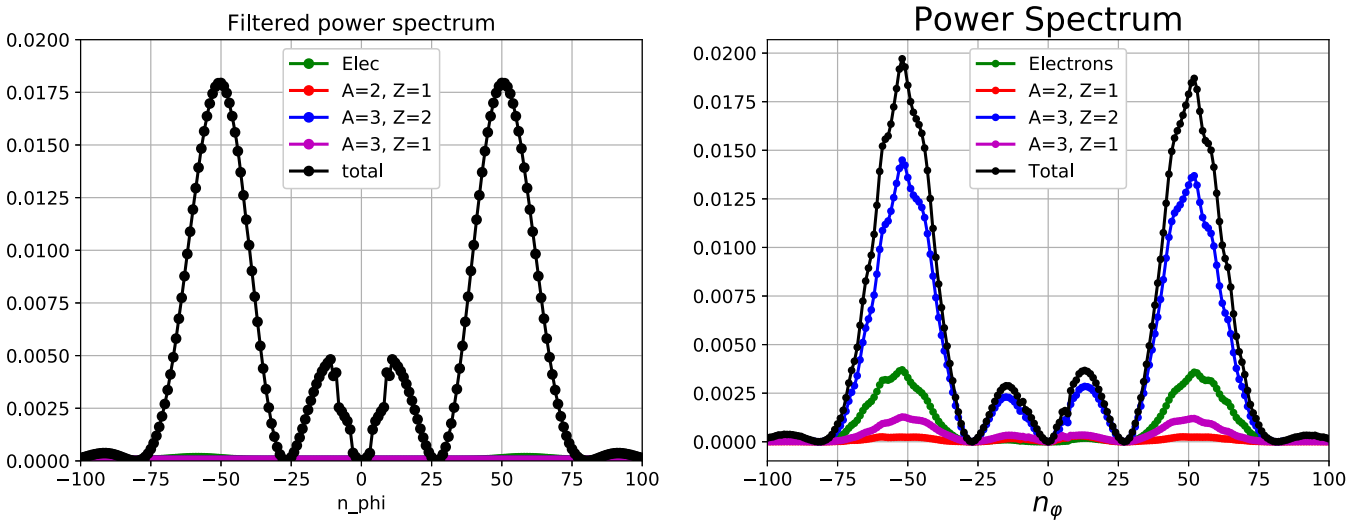

Figure 6. Left: same as figure 5, left, with suppression of the spurious guided modes. Right: the toroidal power spectrum calculated by TORIC for the same ITER scenario.

4. 1D and two-dimensional quasilinear kinetic equations

A further limitation of solvers of Maxwell's equations in plane-stratified geometry is the difficulty of taking into account in a self-consistent way the effects of heating on the distribution functions. As a consequence, these codes usually assume Maxwellian distributions, or use QL distributions chosen with qualitative criteria, for example anisotropic Maxwellians. As mentioned in the introduction, there are two reasons for this limitation:

- A consistent simultaneous determination of the power absorption profiles and of the QL distribution functions requires mapping the profiles obtained in slab geometry onto the magnetic surfaces of the real configuration. Before the advent of computers sufficiently powerful to allow routine simulations in toroidal geometry, this has been attempted, e.g. [28, 29]; it is clear, however, that there is no rigorous quantitative solution of this problem.
- Even if a reasonable way of performing this mapping were found, coupling of slab codes with a solver of the QL kinetic equation is compatible with the speed of execution which is their main advantage only if the latter is also made 1D by integrating the equation over the parallel degree of freedom, a simplification very difficult to justify (in this section one and two dimensions will refer to velocity space).

Figure 7 illustrates the first of the point just raised. In TORIC the power deposited in each species on each magnetic surface is evaluated in W cm^{-3} per MW coupled. The corresponding plot from FELICE is in arbitrary units, since a slab geometry code has no information about the specific volume of

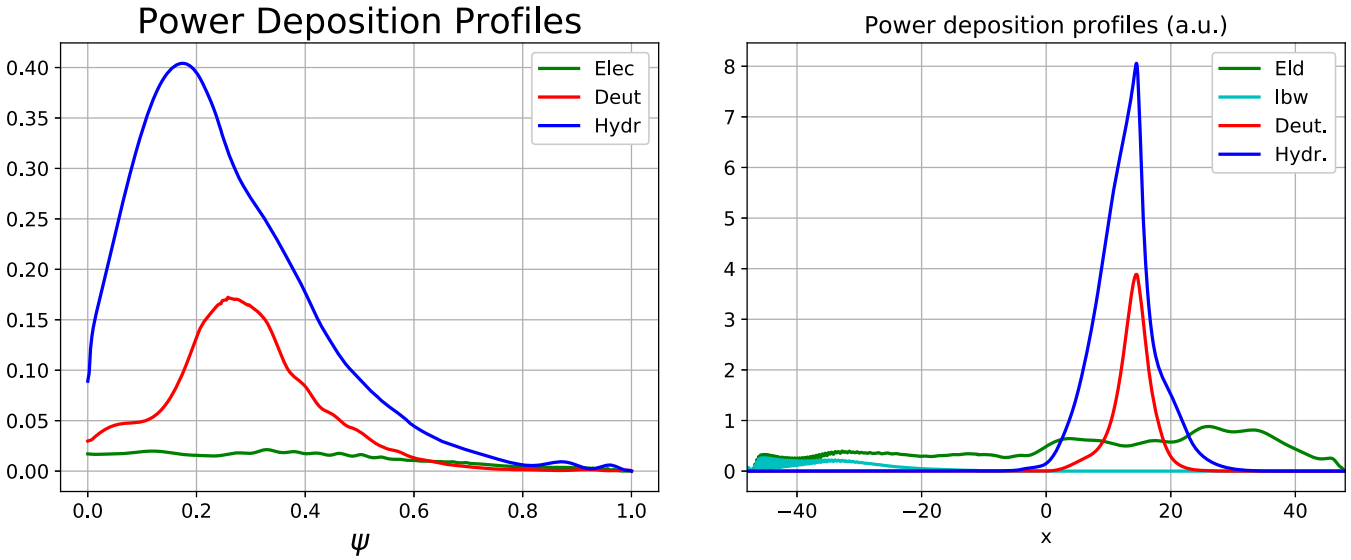

Figure 7. Power deposition profiles, $n_H/n_e = 0.03$. Left TORIC (W cm^{-3} per MW coupled); right: FELICE, arbitrary units.

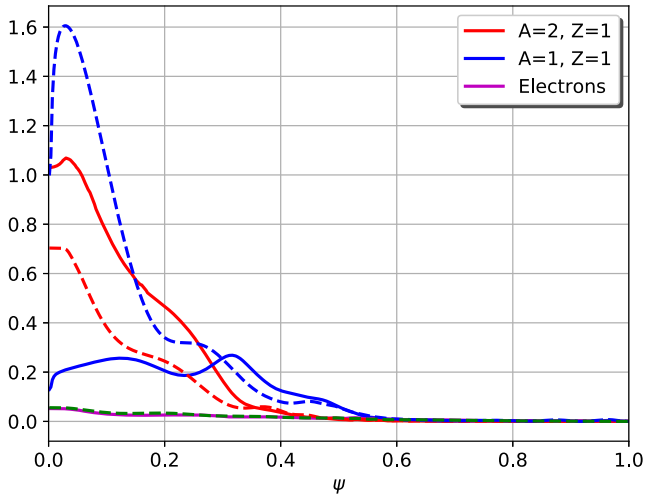

Figure 8. Power deposition profiles: dashed lines in a Maxwellian plasma; full lines at convergence. The abscissa is in W cm^{-3} per MW coupled.

magnetic surfaces. Without precise information on the power absorbed per ion at each magnetic surface there is no reliable way of evaluating the QL ion distribution functions, and the task of imposing consistency between the power absorption profiles calculated by the wave solver and the profiles of QL heating rate cannot be formulated properly.

The 1D kinetic equation, moreover, has very serious limitations itself. To illustrate this we have taken advantage of the fact that SSFPQL has a module which integrates the 1D kinetic equation using the isotropic part of the complete QL diffusion coefficient, for comparison with the results of the full 2D simulation. To make this comparison understandable, it is necessary to briefly recall how consistency between TORIC and SSFPQL is achieved by iterating between the two codes [19, 20]. Initially, TORIC is run (either for a single representative toroidal mode or for the entire toroidal spectrum) assuming Maxwellian distribution functions for all ion species. The resulting power deposition profiles are then used by SSFPQL for a first evaluation of the QL distribution functions on a sufficient number of magnetic surfaces (100 in the example used for this note). For this purpose, the theoretical factor proportional to $|E_+|^2$ of the QL diffusion coefficient D_{ql} is 'adjusted' so that the heating rates predicted by SSFPQL will coincide with the power deposition predicted by TORIC on each magnetic surface of the radial mesh of SSFPQL. These QL distribution functions are used to recalculate the coefficients of the wave equations on these surfaces; a simple and fast algorithm has been developed to evaluate the singular integrals of the Hilbert transforms required for this purpose [41] (cf also the comments on the generalized plasma dispersion function (GPDF) and figure 11 at the end of this section). These coefficients are then interpolated with cubic splines on the much finer radial mesh of TORIC at the next run of this code. This scheme, which requires two runs of SSFPQL for each run of TORIC, is repeated until the power profiles predicted by the two codes agree within an accuracy decided by the user; convergence is accelerated using a variant of the Anderson method [42, 43], specifically adapted to this problem [21]. Note that at convergence the coefficient of D_{ql} calculated as described above would be exactly equal to its theoretical value if no approximations where made in solving both the wave equations and the kinetic equations; since this is of course never possible, this equality is only approximate. It can also be of interest to mention that for the scenario considered here consistency between TORIC and SSFPQL is achieved in five iterations; the two runs of SSFPQL at each iteration execute in about 1 min, while the integration of the 1D linear equation takes much less than 1 ms.

The importance of iterating between TORIC and SSFPQL to reach consistency is clear from figure 8 (in this section the figures are made for the scenario of section 2, but with $f = 36.5$ MHz, which brings the IC resonances very close to the magnetic axis, $n_H/n_e = 3\%$, and a total power of 4 MW). Since first harmonic heating of deuterium is a finite Larmor

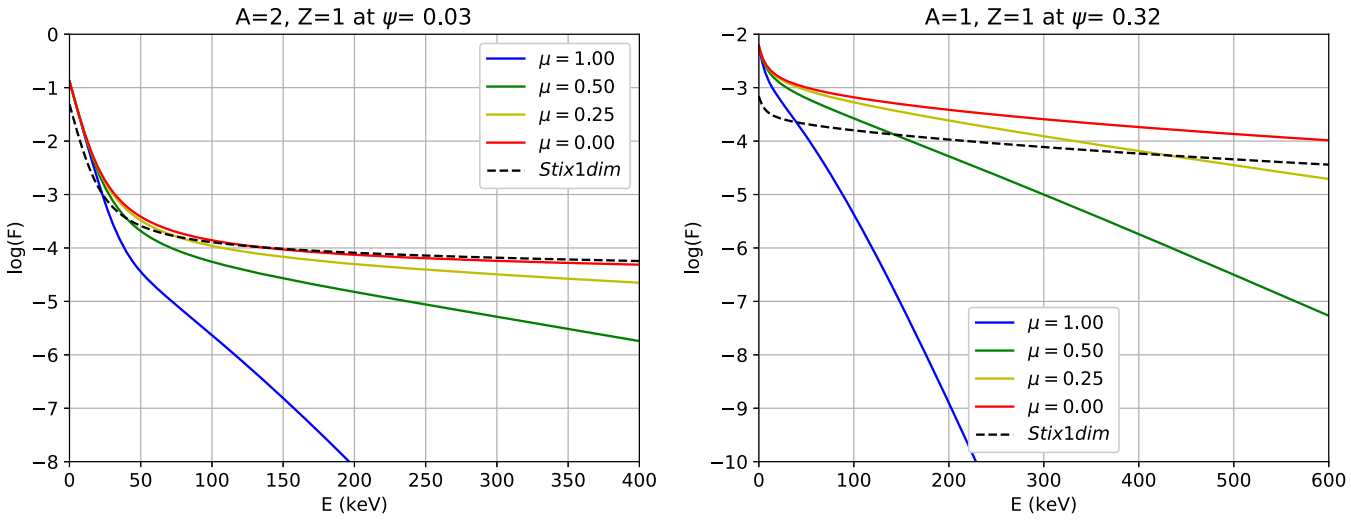

Figure 9. Logarithmic plots of the distribution function at convergence, at the point of highest power absorption. Left: deuterium, right: hydrogen, The black dashed curves are the solution of the 1D kinetic equation. $\mu = v_\parallel^2/v_\perp^2$.

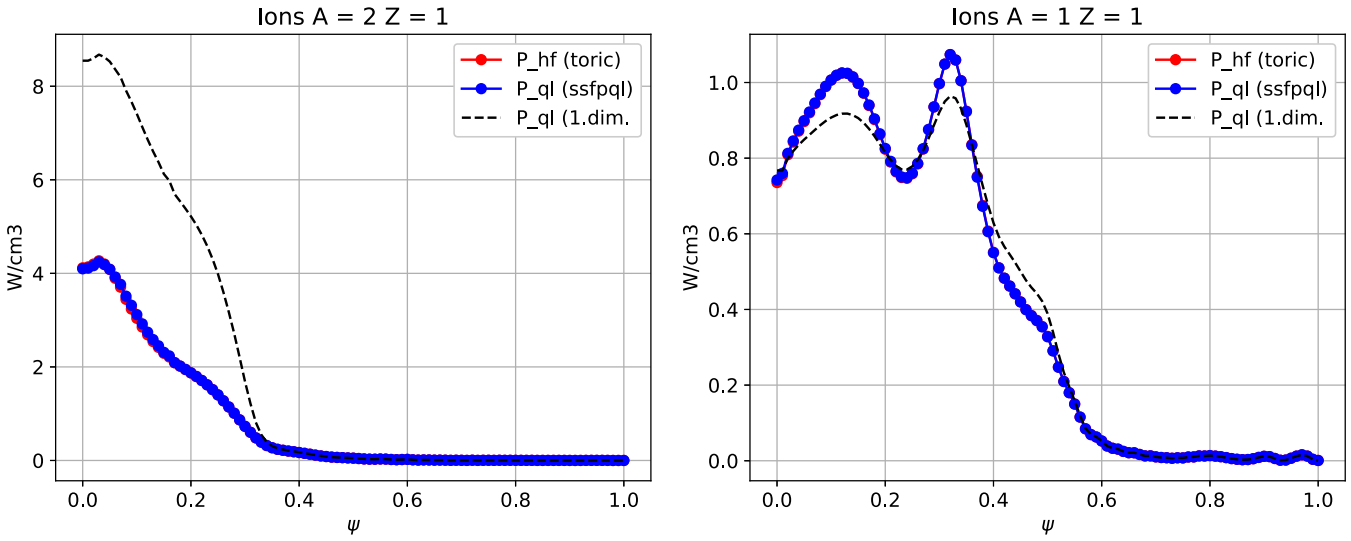

Figure 10. Power deposition profiles at convergence, left: deuterium, right: hydrogen (these plots are for 4 MW total RF coupled power).

radius effect, it is boosted by the development of the suprathermal tail. In this case the effect is so large that much less power reaches the axis, nearly suppressing the central peak of fundamental IC heating of the minority. The broadening of the Doppler width of the resonances due to fast ions is also clearly visible for both species. Simulations without iteration would be clearly misleading (although somewhat less so in ITER or DEMO, where much less RF power per ion will be available; this, however, will be partly compensated by the much lower collisionality).

Since the module of SSFPQL that integrates the 1D kinetic equation uses $D_{\rm ql}$ renormalized by SSFPQL at each iteration, the comparison of the results of the 1D kinetic model with those of SSFPQL makes sense only once convergence between SSFPQL and TORIC is reached, so that the amplitude of the QL diffusion coefficient is as close as possible to its theoretical value (note that these distributions are mapped to the IC resonance; the mapping transforms away the well-known 'rabbit ears' which are present at the outer equatorial point where the distributions are actually calculated). The 1D QL distribution functions are quite similar to the 2D ones for $v_\parallel^2/v_\perp^2 = 0$ (figure 9). This is not surprising, but one should not overlook that if the usual formulas for the QL heating rates are naively applied to the 1D distributions, the radial power absorption profile predicted for the minority is only moderately distorted, but the profile of the majority is higher by a factor two compared to that predicted by TORIC and SSFPQL (which at convergence coincide, figure 10).

More important in the present context is that the output of a 1D solver of the kinetic equation does not allow to take into account that absorption by ions at IC harmonics depends critically mainly on the perpendicular energy content of the distribution functions, while the Doppler broadening of the IC absorption layers, particularly important for minority

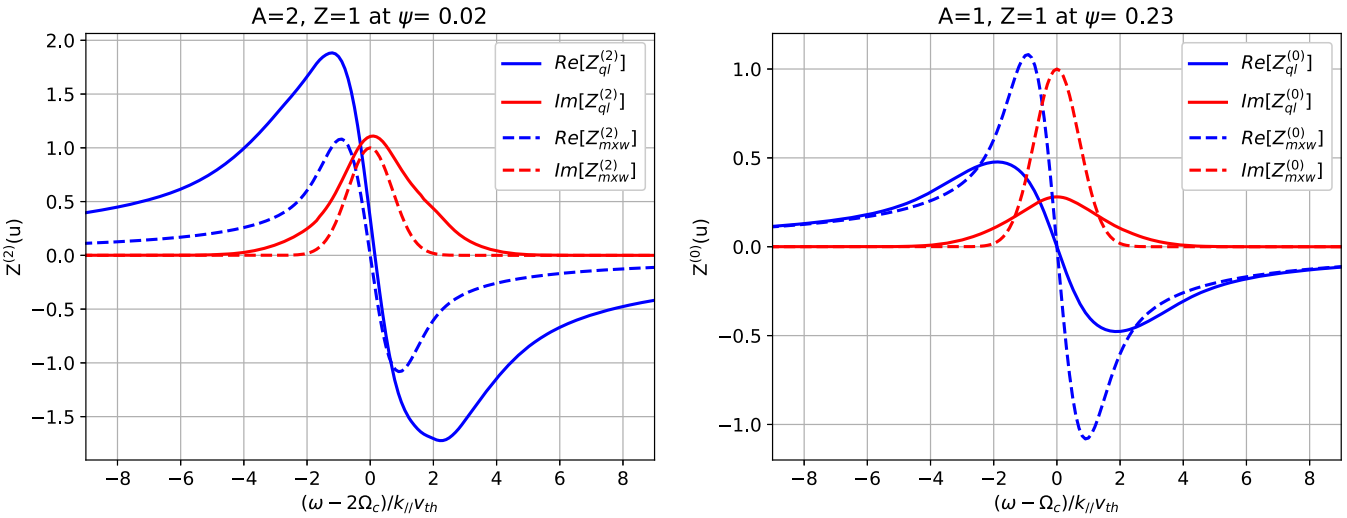

Figure 11. The GPDF passed by SSFPQL to TORIC at the last iteration of the consistency loop, for deuterium (left), and hydrogen (right), at the radial position near the maximum power absorption. This simulation differs from that of figure 9 because we have take into account also 4.86 MW of NBI injection in Deuterium (largest energy channel 60 keV), whose effects are visible in the slight asymmetry of the Deuterium GPDF. The GPDF of Hydrogen is symmetric, because the thermal bath model of collisions does not allow to estimate the indirect effect of the skewness of the deuterium distribution on the Hydrogen.

heating, depends only on the parallel energy content. The importance of this distinction is illustrated by figure 11, which compares the GPDF at the point of maximum power absorption for the two ion species to the Maxwellian plasma dispersion functions of the non RF-heated plasma at the same point.

Figure 11 also indicates that using the so-called 'equivalent Maxwellian' to simulate the effects of a suprathermal population on the coefficients of the wave equations, as is occasionally done when only a code solving the wave equations in Maxwellian plasmas is available, is unlikely to give always satisfactory results. We have proved this quantitatively in [14] for the case of thermonuclear alpha particles in slowing-down.

5. Conclusions

In conclusion, codes solving the wave equations in plane-stratified geometry are important as constituents of antenna codes, and, if used with care, can be useful for a first rapid but qualitative orientation about unfamiliar scenarios. Serious simulations of present day IC heating experiments or of proposed IC heating scenarios for ITER or DEMO, on the other hand, should always be performed with modern wave solvers in full toroidal geometry, which contain (almost) all the required physics, and are coupled to solvers of the QL kinetic equations, so that they can evaluate self-consistently the deviations of the distribution functions from Maxwellian due to resonant interactions with the waves, and the influence of these deviations on the profiles of the power deposition by the waves.

As anticipated in the introduction, we are of course aware that also the models solved by the best toroidal packages are not really 'complete'. Leaving aside the investigation of the fate of the few (but important) most energetic ions whose orbits cannot be regarded as lying on a single magnetic surface and their interactions with the rest of the plasma [44], which is outside the scope of the bounce-averaged QL kinetic equation, in our opinion two problems remain open.

- The first concerns the effects of a (nearly) steady-state ambipolar potential. In toroidal geometry the anisotropy of the energetic tails of the QL ion distribution functions implies that the ion density (and the average energy) will be functions of the poloidal angle. To allow the electrons to maintain charge neutrality an electrostatic potential also depending on ϑ must therefore develop [45]. Heuristic estimates suggest that the amplitude of its variations on each magnetic surface can be a sizeable fraction of the electron temperature, probably sufficient to appreciably modify the unperturbed ion orbits which are used to evaluate the response of the plasma to the waves, and the QL diffusion coefficient in the QL operator.
- The second problem is our more or less complete ignorance of the loss term to be inserted in the kinetic equation in order to guarantee the existence of a steady state solution in the presence of the RF heating source, as observed in the experiments if the heating pulse is sufficiently long. In SSFPQL fast ion losses are simulated by a thermal bath: the exact collisional operator, which conserves energy, is replaced by collisions with a Maxwellian background, which has an infinite heat capacity. The thermal bath model is acceptable when heating rate and collisional relaxation are sufficiently faster than radial diffusion losses; since the latter are poorly known and much dependent on the scenario (collisionality, level of turbulence), however, it is difficult to assess precisely its range of validity. An additional difficulty is that during the heating pulse the bath temperature is not always unambiguously defined. For obvious reasons, on the other hand, it is extremely difficult to devise a loss term reliably describing

losses due to radial diffusion in a wide range of situations. Indeed, by playing with a phenomenological energy loss time one can almost always make the prediction of a kinetic solver agree with the results of a particular experiment; but, lacking a theoretical basis, whether the same loss term will be the correct one for the simulation of future experiments remains completely open. Coupling the solvers of Maxwell's equations and of the QL kinetic equation with a transport code might help, but would not entirely solve the problem, because in the latter radial losses are assumed to depend only on position, while in the kinetic solver it is essential to know in some details their dependence on the energy and velocity pitch angle of the ions (energetic ions on trapped orbits are likely to diffuse away faster than thermal ions).

These two open problems have received very little attention, probably because they are much more difficult than all those which have already been solved. It goes without saying that neither of them can be attacked in plane stratified geometry.

Acknowledgment

We are grateful to W Tierens and L Colas for allowing us to see their work prior to publication. This work has been carried out within the framework of the EUROfusion Consortium and has received funding from the Euratom research and training programme 2014–2018 and 2019-2020 under Grant Agreement No. 633053. The views and opinions expressed herein do not necessarily reflect those of the European Commission.

References

[1] Jaeger E.F., Berry L.A., D'Azevedo E., Batchelor D.B. and Carter M.D. 2001 *Phys. Plasmas* **8** 1573
[2] Jaeger E.F. *et al* 2006 *Nucl. Fusion* **46** S397
[3] Jaeger E.F. *et al* 2006 *Phys. Plasmas* **13** 056101
[4] Dumont R.J. 2009 *Nucl. Fusion* **49** 075033
[5] Dumont R.J. and Zarzoso D. 2013 *Nucl. Fusion* **53** 013002
[6] Brambilla M. and Krücken T. 1988 *Nucl. Fusion* **28** 1813
[7] Brambilla M. 1999 *Plasma Phys. Control. Fusion* **41** 1
[8] Stix T.H. 1975 *Nucl. Fusion* **15** 737
[9] Sauter O., Vaclavik J. and Skiff F. 1990 *Phys. Fluids* B **2** 475
[10] Brambilla M. 2001 *Plasma Phys. Control. Fusion* **43** 4833
[11] Swanson D.G. 1981 *Phys. Fluids* **24** 2035
[12] Colestock P.L. and Kashuba R.J. 1983 *Nucl. Fusion* **23** 763
[13] Brambilla M. 1989 *Plasma Phys. Control. Fusion* **31** 723
[14] Brambilla M. and Bilato R. 2015 *Nucl. Fusion* **55** 023016
[15] Bilato R., Brambilla M. and Fable E. 2014 *J. Phys.: Conf. Ser.* **561** 012001
[16] Bilato R., Brambilla M. and Poli E. 2014 *Phys. Plasmas* **21** 104502
[17] Brambilla M. and Bilato R. 2006 *Nucl. Fusion* **46** s387
[18] Lee J., Wright J., Bertelli N., Jaeger E.F., Valeo E., Harvey R. and Bonoli P. 2017 *Phys. Plasmas* **24** 052502
[19] Brambilla M. and Bilato R. 2009 *Nucl. Fusion* **49** 085004
[20] Brambilla M. and Bilato R. 2013 *Comput. Phys. Commun.* **184** 2053
[21] Bilato R., Brambilla M., Maj O., Horton L.D., Maggi C.F. and Stober J. 2011 *Nucl. Fusion* **51** 103034
[22] Feng Y., Wolle B. and Hübner K. 1995 *Comput. Phys. Commun.* **88** 161
[23] Messiaen A., Koch R., Weynants R.R., Dumortier P., Louche F., Maggiora R. and Milanesio D. 2010 *Nucl. Fusion* **50** 025026
[24] Van Eester D. and Koch R. 1998 *Plasma Phys. Control. Fusion* **40** 1949
[25] Van Eester D. and Lerche E.A. 2021 *Nucl. Fusion* **61** 016024
[26] Maggiora R., Vecchi G., Lancellotti V. and Kyrytsya V. 2004 *Nucl. Fusion* **44** 846
[27] Lancellotti V., Milanesio D., Maggiora R., Vecchi G. and Kyrytsya V. 2006 *Nucl. Fusion* **46** S476
[28] Morishita T., Fukuyama A., Hamamatsu K., Itoh S.-I. and Itoh K. 1983 *Nucl. Fusion* **27** 1291
[29] Carter M.D., Jaeger E.F. and Batchelor D.B. 1989 *Nucl. Fusion* **29** 2141
[30] Hosea J. *et al* 1979 *Phys. Rev. Lett.* **43** 1802
[31] Messiaen A. and Maquet V. 2020 *Nucl. Fusion* **60** 076014
[32] Shiraiwa S., Wright J.C., Lee J. and Bonoli P. 2017 *Nucl. Fusion* **57** 086048
[33] Brambilla M. 1993 *Plasma Phys. Contr. Fusion* **35** 41
[34] Brambilla M. 1995 *Nucl. Fusion* **35** 1265
[35] Tierens W., Milanesio D., Urbanczyk G., Helou W., Bobkov V., Noterdaeme J.-M., Colas L. and Maggiora R. 2019 *Nucl. Fusion* **59** 046001
[36] https://comsol.com/
[37] Brambilla M. and Ottaviani M. 1985 *Plasma Phys. Control. Fusion* **27** 1
[38] Lin Y. *et al* 2008 *Phys. Rev. Lett.* **101** 235002
[39] Tierens W. and Colas L. Electromagnetic surface waves at steep density gradients, with applications in the ion cyclotron range of frequencies (private communication)
[40] Budny R. *et al* 2012 *Nucl. Fusion* **52** 023023
[41] Bilato R., Maj O. and Brambilla M. 2014 *Adv. Comput. Math.* **40** 1159–68
[42] Anderson D.G. 1965 Iterative Procedures for Nonlinear Integral Equations *J. Assoc. Comput. Machinery* **12** 547–60
[43] Walker H. and Ni P. 2011 *SIAM J. Numer. Anal.* **49** 1715
[44] Weiland M., Bilato R., Geiger B., Schneider P.A., Tardini G., Garcia-Muñoz M., Ryter F., Salewski M. and Zohm H. 2017 *Nucl. Fusion* **57** 116058
[45] Bilato R., Maj O. and Angioni C. 2014 *Nucl. Fusion* **54** 072003